Electronic Supplementary Material (ESI) for Environmental Science: Nano.

Supporting Information

Tuning the effective utilization of adsorption sites in La-MOFs via steric hindrance effect towards enhanced As(III) removal

Deng You[a, b, c], Hui Shi[b, c], Liming Yang[b, c,] Penghui Shao[b, c], Xubiao Luo[b, c*], Kai Yin[a*] and Shenglian Luo[a]

[a] *State Key Laboratory of Chemo/Biosensing and Chemometrics, Hunan University, Changsha 410082, P. R. China*

[b] *Key Laboratory of Jiangxi Province for Persistent Pollutants Control and Resources Recycle, Nanchang Hangkong University, Nanchang 330063, P.R. China*

[c] *National-Local Joint Engineering Research Center of Heavy Metals Pollutants Control and Resource utilization, Nanchang Hangkong University, Nanchang 330063, P.R. China*

*** Corresponding author**

E-mail: luoxubiao@126.com (X. Luo)

E-mail: yinkai@hnu.edu.cn (K. Yin)

Contents

SI 20: Estimates of Langmuir and Freundlich parameter values for the adsorption of As(III) on three absorbents at 298K

SI 21: Estimates of parameter values for the adsorption of As(III) on three absorbents at 298K according to the pseudo-first-order and pseudo-second-order models

SI 1: Materials and methods

p-phthalic acid (*p*-PTA: 99.0%), *m*-phthalic acid (*m*-PTA: 99.0%), *o*-phthalic acid (*o*-PTA: 99.0%), sodium arsenite (90.0%) and monopotassium phosphate (99.5%) were purchased from Sigma-Aldrich. Lanthanum chloride heptahydrate (99.9%) were purchased from J&K Chemical. Sodium hydroxide (99.5%), hydrochloric acid (36-38%), absolute ethyl alcohol (99.7%) and N, N'-dimethylformamide (99.5%) were purchased from West long chemical. A Milli-Q ultrapure water purification system (Millipore, Billerica, MA, resistivity >18.2 MΩ·cm) was used to produce deionized water (DI water). All chemicals were of analytical grade and used as-received. Aqueous solutions were all prepared by DI water.

SI 2: Synthesis of the La-MOFs complex

The La-*p*-PTAs, La-*m*-PTAs and La-*o*-PTAs were fabricated via solvothermal methods. Specifically, La-*p*-PTAs complex was synthesized by adding 4 mmol $LaCl_3.7H_2O$ and 2 mmol ligand *p*-PTA to a 100 mL flask, then 60 mL N, N'-dimethylformamide was added to the flask. Then, the mixture was sonicated for up to 30 min and the solution sealed and placed in an oven at 120 ^oC for 12 h. The precipitate was washed 3 times with ethanol and finally vacuum filtered until no residual solvent remained.

SI 3: Material characterization

The morphology of the materials was observed using Tabs F200X transmission electron microscopy (TEM, FEI, USA) and SSX-550 scanning electron microscope (SEM, Shimadzu, Japan). Fourier transmission infrared spectra (FT-IR, 4000−400 cm^{-1}) were recorded on a NICOLET NEXUS 4700 FT-IR spectrometer (Nicolet, Tacoma Washington, USA). X-ray photoelectron spectroscopy (XPS) was logged by a Kratos XSAM800 spectrometer utilizing Al target (1486.6 eV) X ray source (Kratos, UK). Surface structure parameters (BET Surface, pore volume, and pore diameter) were calculated by using the BJH method (BET, Quantachrome EVO, USA). The distribution of adsorption site was observed by QUANTACHROME Chembet Pulsar Temperature-programmed oxygen reduction (TPD-O_2, Quantachrome, USA) and A-300 Electron Paramagnetic Resonance (EPR, BRUCKNER, Germany). The As(III)

concentrations was measured using inductively coupled plasma mass spectrometry (ICP-MS, ELAN DRC-e, Perkin Elmer, Waltham, MA).

SI 4: Adsorption performance experiments

As(III) solution (20 mL) with initial concentrations ranging from 100 to 600 mg L^{-1} was prepared by dilution of concentrated stock solution with DI water. Adsorption isotherms of As(III) at 25 °C were determined by batch experiments, with an adsorbent dosage of 1.0 g L^{-1} for all experiments. The adsorbed amount (Q_e) for As(III) was calculated using the following:

$$Q_e = \frac{V(C_e - C_0)}{m} \quad (1)$$

where V is the volume of the As(III) solution, m is the mass of the La-MOFs adsorbent, and C_0 and C_e are the initial and equilibrium solution concentrations of As(III), respectively.

Langmuir, Freundlich, Temkin and D-R models were used for fitting the temperature dependent adsorption data.[1, 2] As(III) adsorption kinetics were examined with an initial As(III) concentration of 600 mg L^{-1} and placed under constant stirring to reduce mass transfer resistance. To analyze the effect of solution pH on As(III) adsorption, isotherms were determined for pH values varying from 1.0 to 11.0. Desired pH was obtained via dropwise addition of 0.1 M HCl or 0.1 M NaOH to the solution. Batch adsorption experiments were run in triplicate under stirring at 180 rpm for 24 h. The impacts of competing cations on As(III) (0.01 mol/L) adsorption were evaluated in the presence of NaCl, $NaNO_3$ and NaH_2PO_4 (0.002 mol/L) at certain concentrations. All samples were filtered through 0.45 μm cellulose acetate membranes to separate the La-MOFs complex for analysis of As(III) in solution.

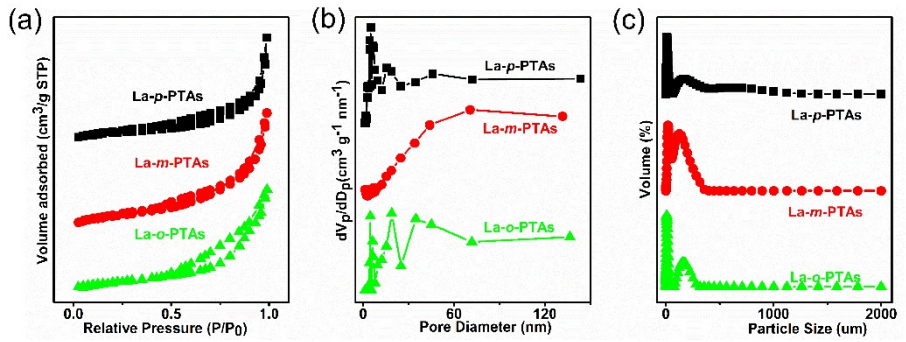

Fig. S1 (a) Nitrogen adsorption-desorption isotherms, (b) pore size distribution and (c) particle size distribution analysis of three La-MOFs.

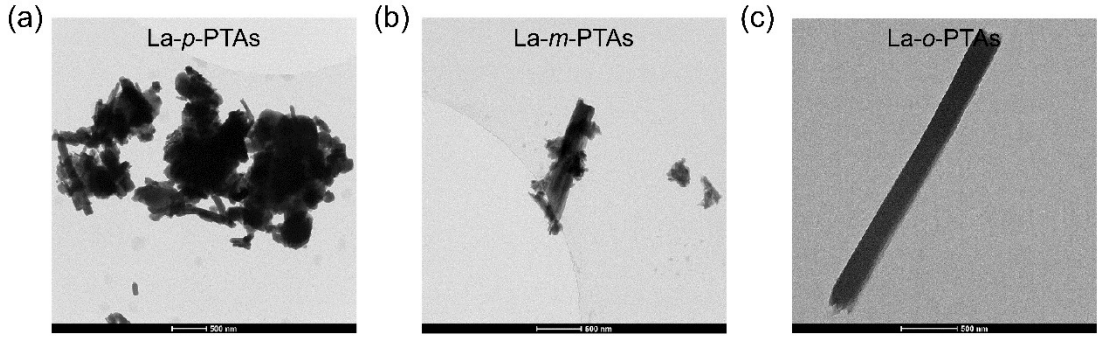

Fig. S2 TEM images of (a) La-*p*-PTAs, La-*m*-PTAs and La-*o*-PTAs at 0.5μm.

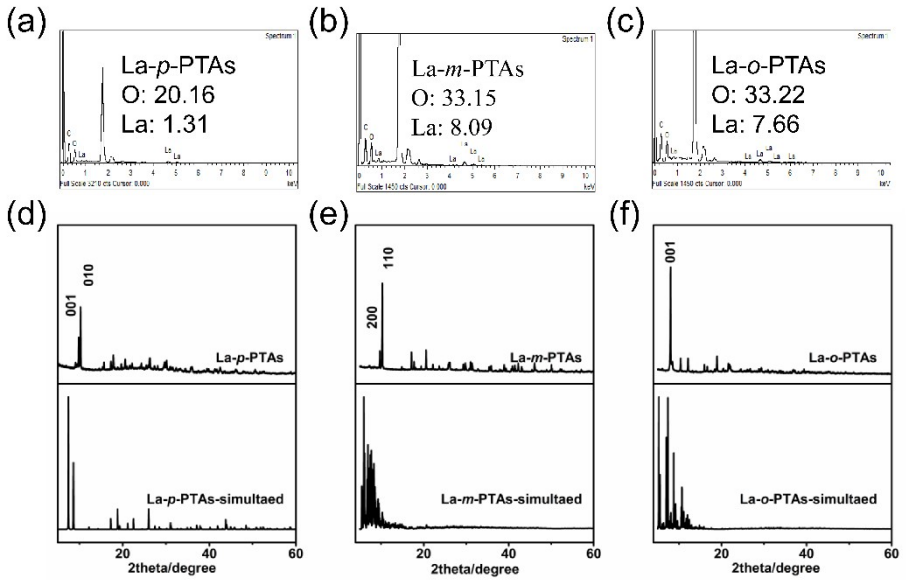

Fig. S3 EDS results of (a) La-*p*-PTAs, (b) La-*m*-PTAs and (c) La-*o*-PTAs. X-ray diffraction (XRD) and corresponding simulated XRD for La-MOFs from rietveld refinement results for (d) La-*p*-PTAs, (e) La-*m*-PTAs and (f) La-*o*-PTAs.

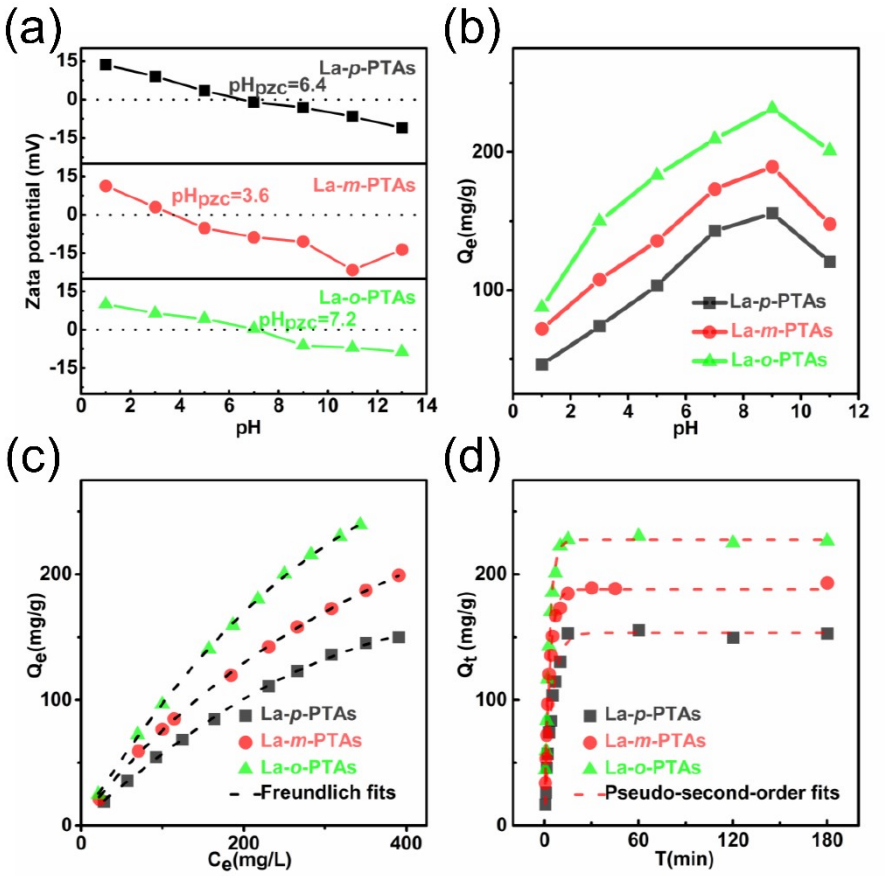

Fig. S4 (a) The zeta potential of three absorbents. (b) Effect of pH on the adsorption capacities of As(III) on different ligand absorbents. The initial As(III) concentrations were 600 mg/L, the adsorbent dose was 1.0 g/L, the solution volume was 30 mL, the pH was 3.0-11.0, and the temperature was 298 K. (c) Adsorption isotherms at 298 K for As(III) onto La-*p*-PTAs, La-*m*-PTAs and La-*o*-PTAs. The adsorbent dose was 1.0 g/L, the solution volume was 30 mL, and the pH was 9. (d) Adsorption kinetics of As(III) absorption onto La-*p*-PTAs, La-*m*-PTAs and La-*o*-PTAs simulated using pseudo-second-order models. The initial concentrations of As(III) was 1 g/L, the adsorbent dose was 1.0 g/L, the solution volume was 400 mL, the pH was 9.0, and the temperature was 298 K.

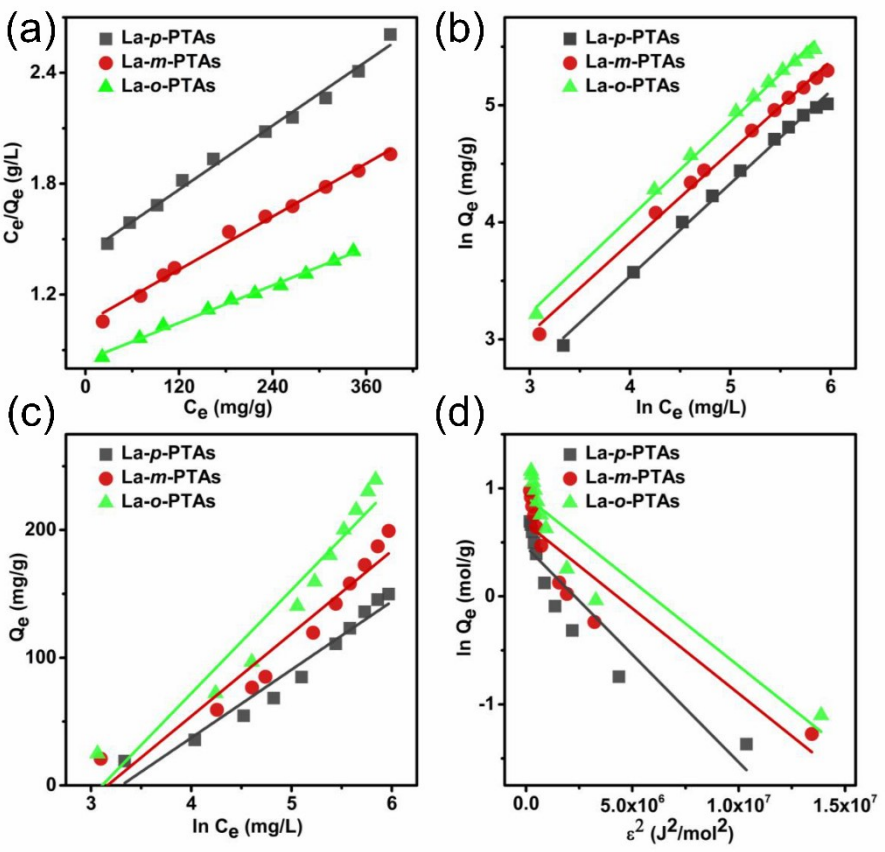

Fig. S5 Adsorption isotherm (a) Langmuir, (b) Freundlich, (c) Temkin, and (d) D-R models for the adsorption of As(III) onto La-*p*-PTAs, La-*m*-PTAs and La-*o*-PTAs.

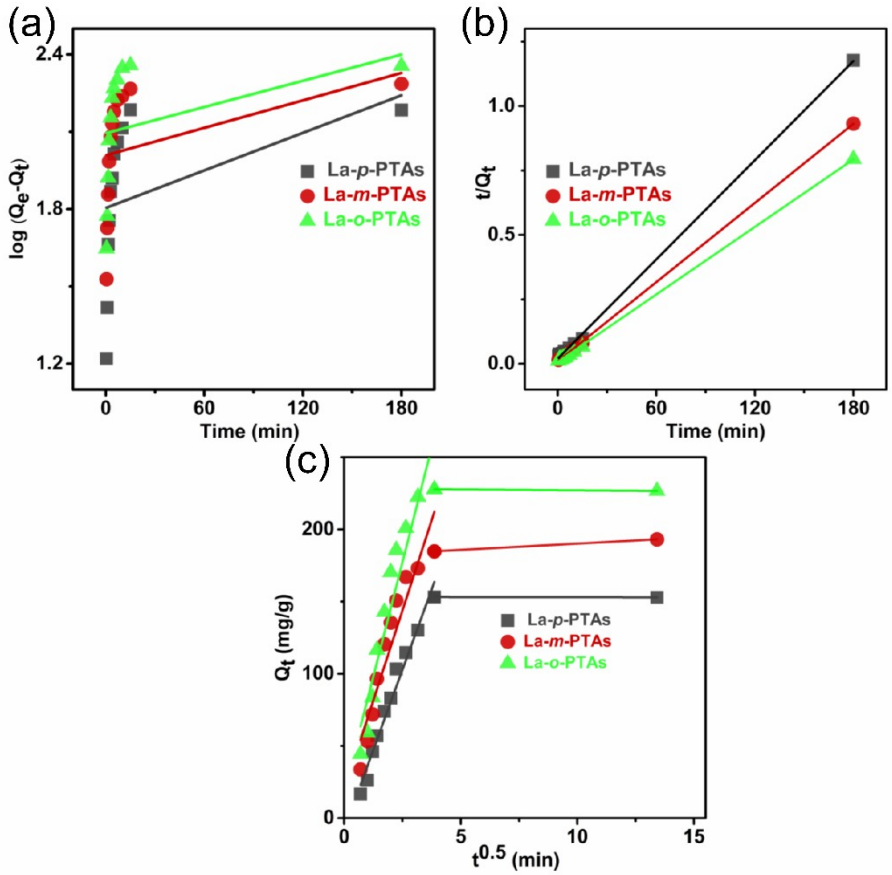

Fig. S6 Kinetic isotherm (a) pseudo-first order, (b) pseudo-second order and (c) intra-particle diffusion kinetic models for As(III) adsorption onto La-*p*-PTAs, La-*m*-PTAs and La-*o*-PTAs.

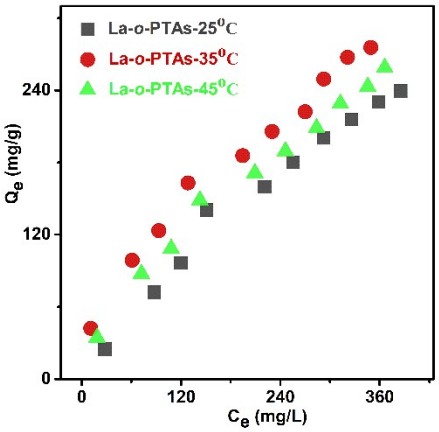

Fig. S7 Adsorption isotherm of As(III) onto La-*o*-PTAs at different temperature.

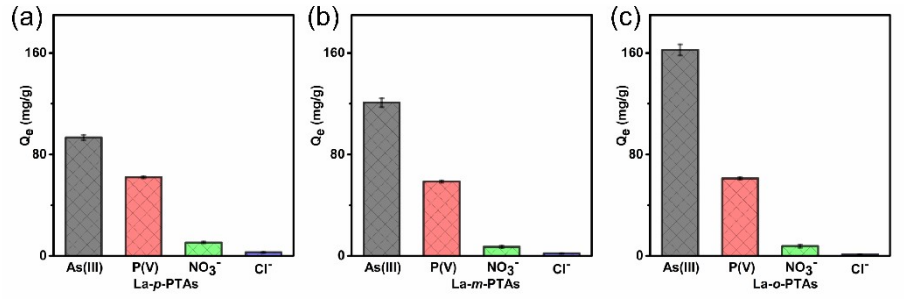

Fig. S8 Effect of competing ions for As(III) adsorption by (a) La-*p*-PTAs, (b) La-*m*-PTAs and (c) La-*o*-PTAs.

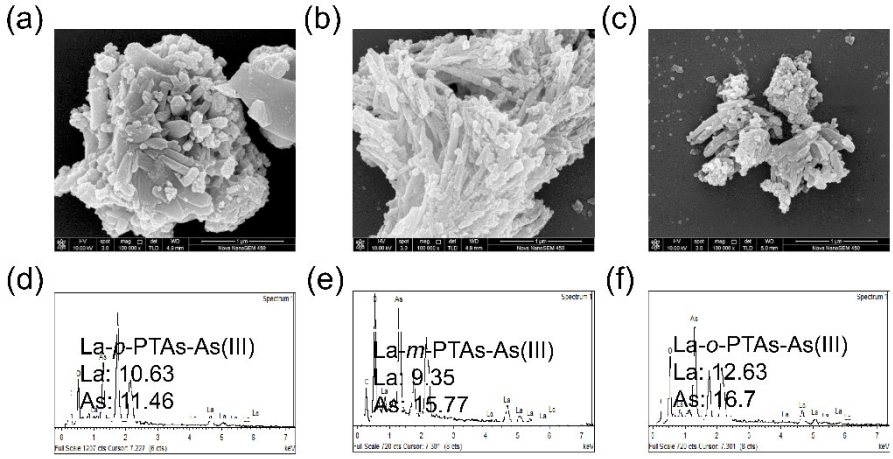

Fig. S9 Scanning electron microscopy (SEM) images of (a) La-*p*-PTAs-As(III), (b) La-*m*-PTAs-As(III), and (c) La-*o*-PTAs-As(III). EDS results of (d) La-*p*-PTAs-As(III), (e) La-*m*-PTAs-As(III), and (f) La-*o*-PTAs-As(III).

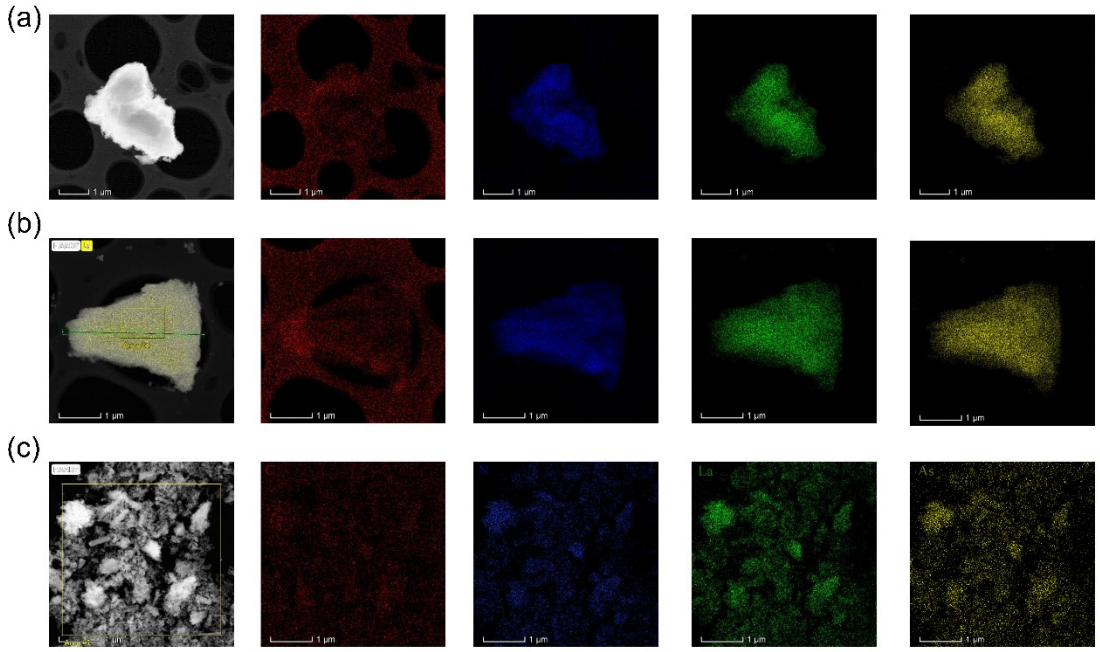

Fig. S10 Elemental mapping images of (a) La-*p*-PTAs-As(III), (b) La-*m*-PTAs-As(III), and (c) La-*o*-PTAs-As(III).

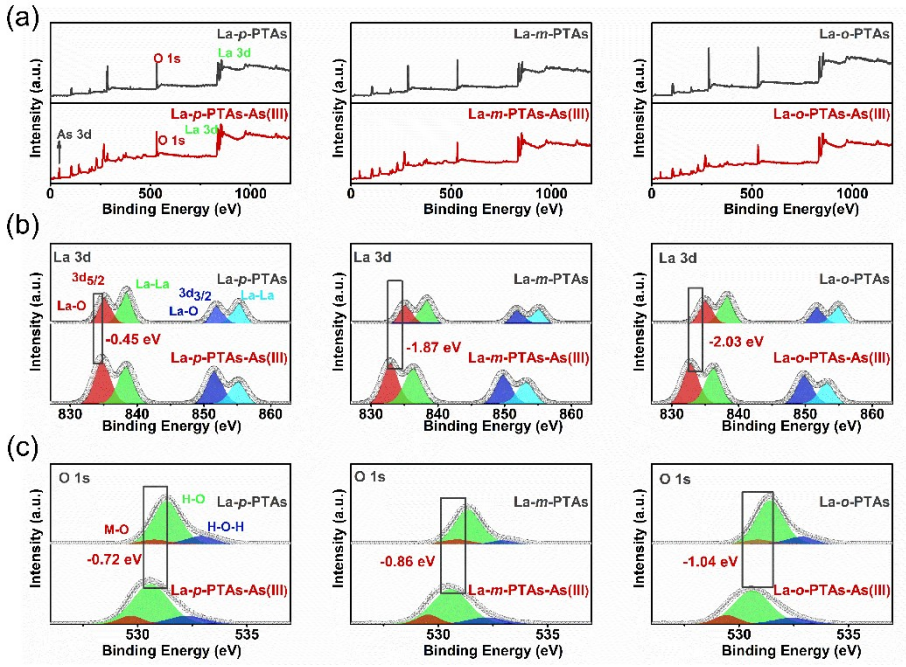

Fig. S11 (a) XPS full spectra, (b) La 3d spectra, and (c) O 1s spectra for La-*p*-PTAs, La-*m*-PTAs and La-*o*-PTAs before and after As(III) absorption.

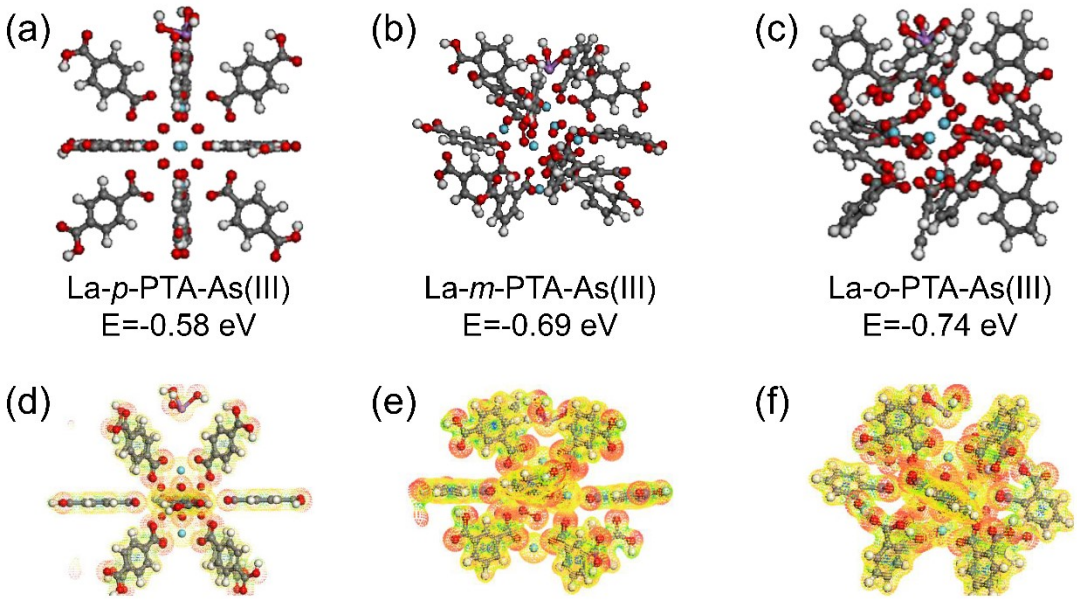

Fig. S12 Theoretical calculations of (a) La-*p*-PTA-As(III), (b) La-*m*-PTA-As(III), and (c) La-*o*-PTA-As(III). Differential electron density distributions of (d) La-*p*-PTA-As(III), (e) La-*m*-PTA-As(III), and (f) La-*o*-PTA-As(III) ranging from 0 to 0.07705 eV. La light blue; O red; C brown; H white and As violet.

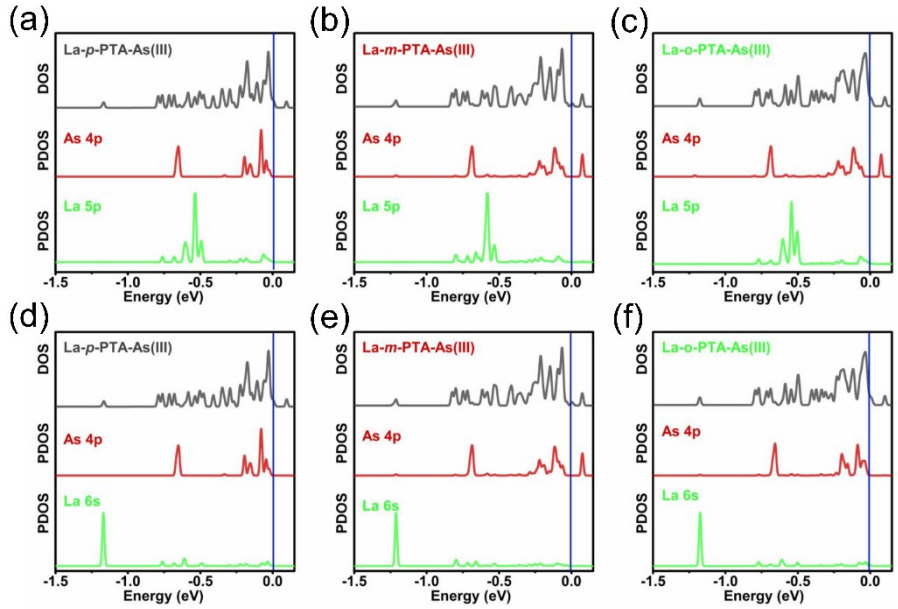

Fig. S13 Density of states and corresponding projected density of states (O 2p, As 4p and La 5p) for (a) La-*p*-PTA-As(III), (b) La-*m*-PTA-As(III), and (c) La-*o*-PTA-As(III). Density of states and corresponding projected density of states (O 2p, As 4p and La 6s) for (d) La-*p*-PTA-As(III), (e) La-*m*-PTA-As(III), and (f) La-*o*-PTA-As(III).

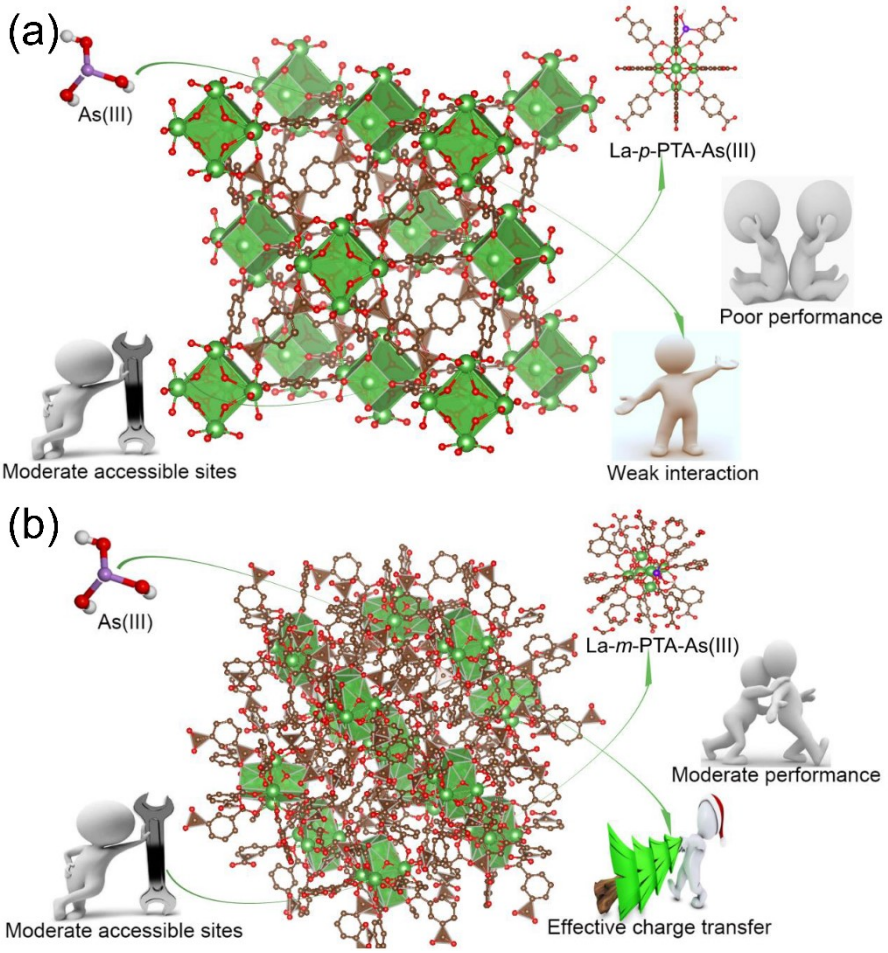

Fig. S14 Mechanism illustrations of (a) La-*p*-PTAs and (b) La-*m*-PTAs for enhanced As(III) absorption.

Table S1. Rietveld refinement results of the La-*p*-PTAs, La-*m*-PTAs, and La-*o*-PTAs from XRD pattern.

Absorbents	La-La distances (Å)	crystal nucleus
La-*p*-PTAs	4.39	10
La-*m*-PTAs	3.31	13
La-*o*-PTAs	3.05	64

Table S2. Estimates of Langmuir and Freundlich parameter values for the adsorption of As(III) on different absorbents at 298K.

Absorbents	Langmuir isotherm parameters			Freundlich isotherm parameters		
	Q_m (mg/g)	K_L(*10^{-3}) (L/mg)	R^2	n	K_F ($mg^{1-(1/n)}L^{1/n}/g$)	R^2
La-*p*-PTAs	346.02	2.03	0.9901	1.08	2.17	0.9997
La-*m*-PTAs	198.41	5.48	0.9934	1.29	2.05	0.9951
La-*o*-PTAs	591.72	2.00	0.9943	1.22	2.15	0.9959

Table S3. Estimates of parameter values for the As(III)adsorption on different absorbents at 298K according to the pseudo-first-order and pseudo-second-order models.

Adsorbate[a]	pseudo-first-order			pseudo-second-order			
	K_1 (min^{-1})	Q_e (mg/g)	R^2	K_2×10^{-3} g/(mg·min)	Q_e (mg/g)	h_0 (mg/g·min)	R^2
La-*p*-PTAs	0.00643	65.70	0.183	2.22	155.5	53.6	0.999
La-*m*-PTAs	0.00453	108.4	0.0818	2.94	195.3	112.0	0.999
La-*o*-PTAs	0.00448	126.9	0.131	3.05	228.8	159.5	0.999

References

1. M. A. Ahsan, V. Jabbari, M. T. Islam, R. S. Turley, N. Dominguez, H. Kim, E. Castro, J. A. H.-Viezcas, M. L. Curry, J. Lopez, J. L. G.-Torresdey, J. C. Noveron, Sustainable synthesis and remarkable adsorption capacity of MOF/graphene oxide and MOF/CNT based hybrid nanocomposites for the removal of Bisphenol A from water, Sci. Total Environ., 2019, 673, 306–317.

2. Md. A. Ahsan, V. Jabbari, M. A. Imam, E. Castro, H. Kim, M. L. Curry, D. J. V.-Rosales, J. C. Noveron, Nanoscale nickel metal organic framework decorated over graphene oxide and carbon nanotubes for water remediation, Sci. Total Environ., 2020, 698, 134214.